The Astrophysical Journal, 578:L67–L70, 2002 October 10

THE SPECTRUM OF THE MASS DONOR STAR IN SS 433

D. R. Gies,[1] W. Huang,[1] and M. V. McSwain
Center for High Angular Resolution Astronomy, Department of Physics and Astronomy, Georgia State University, Atlanta, GA 30303-3083; gies@chara.gsu.edu, huang@chara.gsu.edu, mcswain@chara.gsu.edu
Received 2002 August 1; accepted 2002 August 27; published 2002 September 5

ABSTRACT

We present results from a short series of blue, moderate-resolution spectra of the microquasar binary SS 433. The observations were made at a time optimized to find the spectrum of the donor star, i.e., when the donor was in the foreground and well above the plane of the obscuring disk. In addition to the well-known stationary and jet emission lines, we find evidence of a weak absorption spectrum that resembles that of an A-type evolved star. These lines display radial velocity shifts opposite to those associated with the disk surrounding the compact star, and they appear strongest when the disk is maximally eclipsed. All these properties suggest that these absorption lines form in the atmosphere of the hitherto unseen mass donor star in SS 433. The radial velocity shifts observed are consistent with a mass ratio $M_X/M_O = 0.57 \pm 0.11$ and masses of $M_O = 19 \pm 7\ M_\odot$ and $M_X = 11 \pm 5\ M_\odot$. These results indicate that the system consists of an evolved, massive donor and a black hole mass gainer.

Subject headings: stars: early-type — stars: individual (SS 433, V1343 Aquilae) — X-rays: binaries

1. INTRODUCTION

SS 433 is still one of the most mysterious of the X-ray binaries, even after some 25 years of observation (Margon 1984; Zwitter et al. 1989; Gies et al. 2002). We know that the mass donor feeds an enlarged accretion disk surrounding a neutron star or black hole companion and that a small portion of this inflow is ejected into relativistic jets that are observed in optical and X-ray emission lines and in high-resolution radio maps. There are two basic timescales that control the spectral appearance and system dynamics, a 162 day disk and jet precessional cycle and a 13 day orbital period. The mass function derived from the He II λ4686 emission line indicates that the donor star mass is greater than 8 $M_\odot$ (Fabrika & Bychkova 1990). The donor is probably a Roche-filling, evolved star (King, Taam, & Begelman 2000). However, the spectral signature of this star has eluded detection. This is probably because the binary is embedded in an expanding thick disk that is fed by the wind from the super-Eddington accretion disk (Zwitter, Calvani, & D'Odorico 1991). The outer regions of this equatorial thick disk have been detected in high-resolution radio measurements by Paragi et al. (1999) and Blundell et al. (2001). Many of the properties of the "stationary" emission lines can be explained in terms of a disk wind (Gies et al. 2002).

The task of finding the spectrum of the donor is crucial because without a measurement of its orbital motion, the mass of the relativistic star is unknown. The best opportunity to observe the flux from the donor occurs at the precessional phase when the disk normal is closest to our line of sight and the donor star appears well above the disk plane near the donor inferior conjunction orbital phase (Gies et al. 2002). This configuration occurs only a few nights each year. The choice of spectral region is also important. Goranskii, Esipov, & Cherepashchuk (1998b) found that the regular eclipse and precessional variations seen clearly in the blue are lost in the red because of an erratically variable flux component. Thus, we need to search for the donor spectrum blueward of the *R* band in order to avoid this variable component. On the other hand, the color variations observed during eclipses suggest that the donor is cooler than the central portions of the disk (Antokhina & Cherepashchuk 1987; Goranskii et al. 1997). Thus, the disk will tend to contribute a greater fraction of the total flux at lower wavelengths. The best compromise is in the blue, where there are a number of strong absorption lines in B- and later-type stars.

2. OBSERVATIONS

Blue spectra of SS 433 were obtained on three consecutive nights, 2002 June 5–7, with the Large Cassegrain Spectrograph (LCS) on the 2.7 m Harlan J. Smith Telescope at the University of Texas McDonald Observatory. These dates correspond to precessional phases between $\Psi = 0.998$ and 0.011 (where $\Psi = 0.0$ corresponds to the time when the jets are closest to our line of sight and their emission lines attain their extremum radial velocities) and to orbital phases between $\phi = 0.012$ and 0.178 (where mideclipse and donor inferior conjunction occur at $\phi = 0.0$) according to the phase relations adopted in Gies et al. (2002). The spectra were made in first order with the 46 grating (1200 grooves mm^{-1}, blazed at 4000 Å), and they cover the wavelength range between 4060 and 4750 Å. We used a long-slit configuration with a slit width of 2″.0, which corresponds to a projected width of 2 pixels FWHM on the detector, a 800 × 800 format TI CCD with 15 μm square pixels. The reciprocal dispersion is 0.889 Å pixel^{-1}, and the spectral resolving power is $\lambda/\triangle\lambda = 2500$. Unfortunately, the weather was partially cloudy throughout the run, and we were only able to obtain a few consecutive, 20 minute exposures on each night. We also obtained a full suite of calibration bias, dome flat field, and argon comparison frames throughout the run.

The spectra were extracted and calibrated using standard routines in IRAF.[2] We co-added all the consecutive spectra from a given night to increase the signal-to-noise (S/N) ratio. The co-added spectra were then rectified to a unit continuum by the fitting of line-free regions. Note that this rectification process arbitrarily removes the continuum flux variations that occurred

[1] Visiting Astronomer, University of Texas McDonald Observatory.

[2] IRAF is distributed by the National Optical Astronomy Observatories, which is operated by the Association of Universities for Research in Astronomy, Inc., under cooperative agreement with the National Science Foundation.

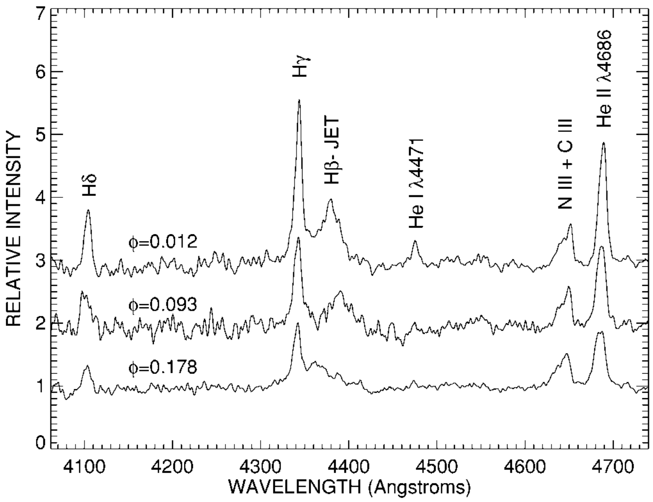

FIG. 1.—Rectified spectra of SS 433 marked with labels for the prominent features. The spectra are shown chronologically from the first night (*upper line*) to the last night (*lower line*), and the spectrum for each night is offset by unity for clarity. The orbital phases of observation, ϕ, are listed above each spectrum.

in SS 433 during the eclipse. All the spectra were then transformed to a common heliocentric wavelength grid for ease of comparison. The final S/N ratios in the continuum at the long-wavelength end of the spectra are 31, 16, and 40 pixel^{-1} for the three consecutive nights, respectively.

3. EMISSION-LINE SPECTRUM

Our three spectra are shown in chronological sequence in Figure 1. This part of the spectrum is dominated by the familiar strong emission lines of Hδ, Hγ, and He II λ4686 (Murdin, Clark, & Martin 1980; Panferov & Fabrika 1997; Fabrika et al. 1997a). The only strong jet emission feature in this spectral range at this time is the blueshifted H$\beta-$ line (formed in the approaching jet), which is found just longward of Hγ. This spectral range should also contain redshifted jet components from the upper Balmer sequence (from the Balmer limit at $\approx$4267 Å to Hϵ at $\approx$4645 Å), but, if present, they are too weak to detect in our spectra. We measured the radial velocity of the H$\beta-$ emission feature by fitting a single Gaussian in each case. These measurements are partially compromised by the appearance of multiple subpeaks in some cases (see the final profile that contains a redshifted, subpeak corresponding in radial velocity to the "bullet" that appeared on the previous night) and by the possible existence of very weak He I λ4387 emission. Nevertheless, these measurements show the familiar oscillations in the jet velocities due to the tidal "nodding" of the accretion disk (Vermeulen et al. 1993; Gies et al. 2002). Table 1 lists the heliocentric Julian Date for the midtime of each observation, the observed H$\beta-$ radial velocity as $z = V_r/c$ (estimated errors ± 0.001), and the predicted z-value based on the extrapolation of the fit to the Hα jet velocities observed between 1998 and 1999 (Gies et al. 2002). The good agreement between the observed and predicted motions suggests that our jet precessional velocity fit is still reliable 3 years after the last Hα observations.

TABLE 1
JET RADIAL VELOCITY MEASUREMENTS

Date (HJD − 2,450,000)	Observed z(H$\beta-$)	Predicted z(H$\alpha-$)
2430.7616	−0.099	−0.098
2431.8226	−0.097	−0.095
2432.9381	−0.103	−0.100

The stationary emission lines generally fall into two categories: (1) lines like He II λ4686 that form in a region symmetric about the center of the accretion disk and that show orbital radial velocity curves of the form $-K_1 \sin(2\pi\phi) + V_1$ and (2) features like the hydrogen Balmer lines that probably form in a large volume in the disk's wind and have a radial velocity variation of the form $K_2 \cos(2\pi\phi) + V_2$ (Gies et al. 2002). We measured the radial velocities of the stationary lines in our spectra to confirm their radial velocity behavior. The profiles were obtained by Gaussian fitting in all cases except for the N III+C III complex near 4644 Å, where we measured relative shifts by cross-correlating the profiles for the second and third nights against that from the first night. Our results are listed in Table 2 (errors are ± 30 km s^{-1}). All the lines showed the blueward motion expected in this phase interval, but with a larger amplitude than predicted. The largest decline was found in N III+C III and He II λ4686, which decreased in radial velocity by $\approx$214 km s^{-1} over the duration of observations ($\phi = 0.01$–0.18). Fabrika & Bychkova (1990) estimate that the disk semiamplitude is $K_1 \approx 175$ km s^{-1}, smaller than we observed. The same situation occurred in lines of the other group, Hδ, Hγ, and He I λ4471, which declined by some 108 km s^{-1} (compared with the expected $K_2 \approx 64$ km s^{-1}; Gies et al. 2002). We speculate that this difference is due to the emergence of the approaching portion of the disk after the eclipse, which biases the radial velocities to more negative values.

The other clue about the origin of the stationary lines comes from their intensity variations during the eclipse. If the emission source has a constant flux, then during eclipse the line will appear proportionally stronger relative to the lower continuum flux. However, if the emission source is also (partially) eclipsed, then the relative strength in rectified intensity remains approximately constant in eclipse. We show in Table 3 the rectified intensities of the emission lines for the first two nights relative to that on the final night. The final column gives the predicted constant emission flux variation relative to the last night based on the *V*-band light curve (Goranskii, Esipov, & Cherepashchuk 1998a; see their Fig. 7*b*) and the $B-V$ color variations (Goranskii et al. 1997; see their Fig. 3). We find that most of the line intensities decreased by a factor of 2.4 between the first (mideclipse) and last (out of eclipse) observations, compared

TABLE 2
STATIONARY LINE RADIAL VELOCITY MEASUREMENTS

Date (HJD − 2,450,000)	V_r (Hδ) (km s^{-1})	V_r (Hγ) (km s^{-1})	V_r (He I) (km s^{-1})	V_r (N III)[a] (km s^{-1})	V_r (He II) (km s^{-1})	V_r (abs.)[a] (km s^{-1})
2430.7616	169	204	264	0	168	0
2431.8226	25	118	204	−96	50	38 ± 35
2432.9381	77	80	157	−216	−44	87 ± 15

[a] Cross-correlation velocity relative to first observation.

TABLE 3
Relative Line Intensities $F_l/F_c : F_l/F_c(\phi = 0.178)$

Orbital Phase	Hδ	Hγ	He I	N III	He II	Hβ−	Absorption[a]	*B* Light Curve[b]
0.012	2.28	2.53	2.47	1.20	2.16	2.44	2.6	1.91
0.093	1.58	1.38	1.56	1.16	1.40	1.25	1.5	1.22

[a] Cross-correlation intensity relative to that at phase 0.178.
[b] Prediction for constant F_l relative to phase 0.178.

with the predicted decrease of a factor of 1.9 for a constant emission flux source. This difference is probably not significant since the intrinsic system flux varies on short timescales, but the result does suggest that most of the lines form in regions large compared with the continuum-forming part of the accretion disk (so that the continuum-forming inner disk is eclipsed while the much larger line-forming region suffers only minor occultation). The main exception is the N III+C III line, which varies little in rectified intensity and must therefore form cospatially with the continuum in the inner, hot part of the accretion disk. The other possible exception is the line He II λ4686. Goranskii et al. (1997) and Fabrika et al. (1997b) observed profile shape variations during the eclipse that we also find (for example, from single- to double-peaked with egress from the eclipse), and they argue that the feature has two components, one formed in gas close to the disk center (eclipsed) and one formed in a larger volume (not eclipsed). This assessment agrees with the fact that after the N III+C III line, the He II λ4686 feature shows the second smallest decrease in rectified flux, suggesting that its line-forming region is more occulted during the eclipse than is the case for the H and He I lines (formed in the larger disk wind).

4. ABSORPTION-LINE SPECTRUM

In comparing the individual spectra, we were struck by the similarity of patterns of what might first be considered "noise" in the continuum between the strong emission lines. We formed a global average spectrum, with each spectrum weighted by the square of its S/N ratio, and an expanded version of this average spectrum is shown in Figures 2 and 3. Below the average SS 433 plot, we show examples of stellar spectra that could correspond to the spectral type of the donor star. The two B-type star spectra were selected from the atlas of Walborn & Fitzpatrick (1990), and we obtained the spectrum of the A-type supergiant, HD 148743, with the LCS. All these spectra were Gaussian-smoothed to an effective 2 pixel resolution of 1.78 Å FWHM in order to compare them at the same instrumental resolution. We see that there is a significant (and largely unresolved) system of absorption lines in SS 433 that has eluded detection in earlier work. The line patterns bear little resemblance to those in B-type supergiants, but there are a number of features in common with the A-type supergiant ($T_{\rm eff} = 7800$ K; Venn 1995). We show some preliminary identifications of the absorption lines based on lists in Ballereau (1980) and Venn (1995).

We measured the radial velocity of the absorption system by cross-correlating subsections of the spectrum containing the deepest features with those in the first spectrum of the set. These relative velocities are listed in the final column of Table 2. (We found that the absorption lines in the first spectrum had a cross-correlation velocity of -39 ± 20 km s^{-1} compared with the rest-frame spectrum of HD 148743, so adding this value to the velocities in Table 2 gives an estimate of the absolute velocities.) Unlike the emission lines, the absorption lines moved significantly redward during the run, as expected for the donor star.

Direct inspection of Figure 1 suggests that the absorption-line spectrum grew fainter with egress from the eclipse, as predicted for the donor's spectrum. It is difficult to measure the change in individual lines, so we measured the strength of the cross-correlation of the absorption lines with those in HD 148743. The relative cross-correlation intensities are listed in the second to last column of Table 3 (errors of ± 0.5). The absorption depths weakened in the same way as the emission

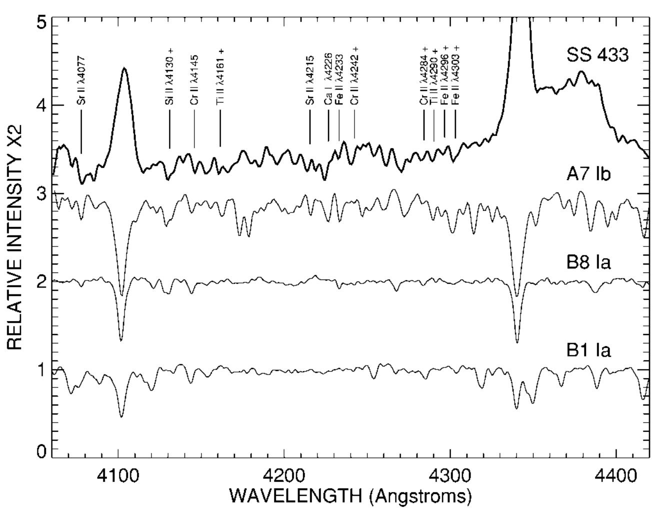

Fig. 2.—Detailed plot of the lower wavelength portion of the co-added spectrum of SS 433 (*thick line*). The individual spectra were shifted to the rest frame prior to co-addition. Several examples of the predicted donor spectrum are shown below (*thin lines*): HD 148743 (A7 Ib), β Ori (B8 Ia), and HD 148688 (B1 Ia). All the spectral intensities were increased by a factor of 2 and offset in intensity for ease of comparison. Preliminary identifications are given for a number of weak absorption lines in the spectrum of SS 433. A plus sign following the identification indicates a blend of multiple lines.

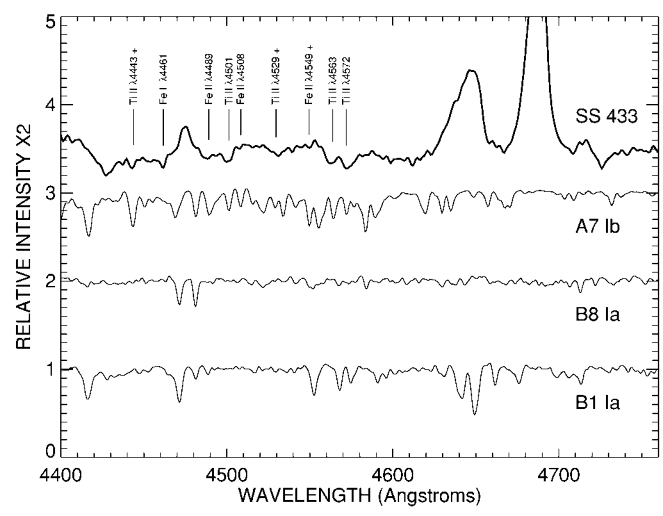

Fig. 3.—Detailed plot of the longer wavelength portion of the co-added spectrum of SS 433 in the same format as Fig. 2.

intensities, suggesting that both became diluted by the emerging flux of the disk.

Both the radial velocity and intensity variations indicate that the absorption lines form in the long-sought donor star. If they were formed in the interstellar medium (the case of the absorptions at 4428, 4501, and 4726 Å), then we would observe no velocity or intensity variations through these eclipse phases. Similar arguments rule out formation in an extended "shell" surrounding the binary system.

The absorption-line velocities are insufficient for a general orbital solution, but we can make a restricted solution if we assume that the orbit is circular and if we adopt the orbital period and epoch of mideclipse from Goranskii et al. (1998a). Then we can solve for two parameters, the systemic velocity, V_0, and orbital semiamplitude, K_O, from our three radial velocity measurements of the optical star. We used the orbital fitting code of Morbey & Brosterhus (1974) to find $V_0 = -44 \pm 9$ km s^{-1} and $K_O = 100 \pm 15$ km s^{-1} with residual errors of 9 km s^{-1}. Fabrika & Bychkova (1990) find that the semiamplitude of the disk is $K_X = 175 \pm 20$ km s^{-1} based on the He II λ4686 radial velocity curve (corresponding to the motion of the compact star at the center of the X-ray source). They adopt the system inclination from the "kinematical" model of the jets to arrive at a mass relation, $M_O/(1+q)^2 = 7.7 \pm 2.7\ M_\odot$, where the mass ratio is $q = M_X/M_O$. We can now combine the semiamplitudes to estimate the mass ratio, $q = K_O/K_X = 0.57 \pm 0.11$ (more consistent with models of the optical light curve than those of the X-ray light curve; Antokhina & Cherepashchuk 1987; Antokhina, Seifina, & Cherepashchuk 1992; Gies et al. 2002). The resulting masses are $M_O = 19 \pm 7\ M_\odot$ and $M_X = 11 \pm 5\ M_\odot$, which suggests that the companion is a black hole.

The metal absorption lines strengthen from main sequence to supergiant in the A-type stars, and they appear sufficiently strong in the first eclipse spectrum to rule out a main-sequence class. The donor star probably fills its critical Roche surface, and our estimate of the mass ratio indicates a Roche volume radius of $31 \pm 3\ R_\odot$, consistent with a supergiant class. Thus, our results for SS 433 support the evolutionary scenario described by King et al. (2000) in which mass transfer is occurring on a thermal timescale as the donor crosses the Hertzsprung gap.

We can estimate the magnitude difference between the star and the disk, $\triangle B$, based on the apparent line depths. Let us suppose that during the central eclipse, a disk flux F_1 is occulted while a disk flux F_2 and donor star flux $F_\star$ remain visible. The stellar line depths will then appear diluted by a factor $F_\star/(F_2 + F_\star)$. The observed line depths during eclipse (relative to the spectrum of the A-type supergiant) suggest that dilution is minimal, so $F_2/F_\star = 0$–1. Based on the line intensity variations that we observed (Table 3), the ratio of out-of-eclipse to mideclipse flux is 2.38 ± 0.15, and thus the ratio of disk to star flux is $(F_1 + F_2)/F_\star = 1.4$–2.8 (or $\triangle B = 0.3$–1.4 mag). A donor star this bright may appear to be in conflict with earlier results (Antokhina & Cherepashchuk 1987; Goranskii et al. 1998a; Gies et al. 2002), but we suspect that the star is heavily obscured at other precessional and orbital phases so that its line spectrum is difficult to find (and estimates of the donor star's flux based on the absence of the lines will be too low).

Clearly our results should be regarded as preliminary since we have only observed the absorption spectrum during this one eclipse, and SS 433 is known to display spectroscopic variations on timescales unrelated to the orbit. Nevertheless, confirmation of our results (especially in spectra of higher S/N ratio and resolution) would be of particular importance in determining the stellar parameters of the donor ($T_{\rm eff}$, log g, and abundance) and in refining the mass estimates. We emphasize again that the successful detection of the donor spectrum is probably limited to times near $\Psi = 0$ and $\phi = 0$. The next opportunities will occur near 2002 November 10, 2003 April 28, and 2003 October 2.

We are grateful to Anita Cochran and the staff of the McDonald Observatory for their help. Support for this work was provided by NASA through grant GO-8308 from the Space Telescope Science Institute, which is operated by the Association of Universities for Research in Astronomy, Inc., under NASA contract NAS5-26555. Institutional support has been provided from the GSU College of Arts and Sciences and from the Research Program Enhancement fund of the Board of Regents of the University System of Georgia, administered through the GSU Office of the Vice President for Research. We gratefully acknowledge all this support.

REFERENCES

Antokhina, E. A., & Cherepashchuk, A. M. 1987, Soviet Astron., 31, 295
Antokhina, E. A., Seifina, E. V., & Cherepashchuk, A. M. 1992, Soviet Astron., 36, 143
Ballereau, D. 1980, A&AS, 41, 305
Blundell, K. M., Mioduszewski, A., Muxlow, T. W. B., Podsiadlowski, P., & Rupen, M. 2001, ApJ, 562, L79
Fabrika, S. N., & Bychkova, L. V. 1990, A&A, 240, L5
Fabrika, S. N., Goranskij, V. P., Rakhimov, V. Y., Panferov, A. A., Bychkova, L. V., Irsmambetova, T. R., Shugarov, S. Y., & Borisov, G. V. 1997a, Bull. Spec. Astrophys. Obs., 43, 109
Fabrika, S. N., Panferov, A. A., Bychkova, L. V., & Rakhimov, V. Y. 1997b, Bull. Spec. Astrophys. Obs., 43, 95
Gies, D. R., McSwain, M. V., Riddle, R. L., Wang, Z., Wiita, P. J., & Wingert, D. W. 2002, ApJ, 566, 1069
Goranskii, V. P., Esipov, V. F., & Cherepashchuk, A. M. 1998a, Astron. Rep., 42, 209
———. 1998b, Astron. Rep., 42, 336
Goranskii, V. P., Fabrika, S. N., Rakhimov, V. Yu., Panferov, A. A., Belov, A. N., & Bychkova, L. V. 1997, Astron. Rep., 41, 656
King, A. R., Taam, R. E., & Begelman, M. C. 2000, ApJ, 530, L25
Margon, B. 1984, ARA&A, 22, 507
Morbey, C. L., & Brosterhus, E. B. 1974, PASP, 86, 455
Murdin, P., Clark, D. H., & Martin, P. G. 1980, MNRAS, 193, 135
Panferov, A. A., & Fabrika, S. N. 1997, Astron. Rep., 41, 506
Paragi, Z., Vermeulen, R. C., Fejes, I., Schilizzi, R. T., Spencer, R. E., & Stirling, A. M. 1999, A&A, 348, 910
Venn, K. A. 1995, ApJS, 99, 659
Vermeulen, R. C., et al. 1993, A&A, 270, 204
Walborn, N. R., & Fitzpatrick, E. L. 1990, PASP, 102, 379
Zwitter, T., Calvani, M., Bodo, G., & Massaglia, S. 1989, Fundam. Cosmic Phys., 13, 309
Zwitter, T., Calvani, M., & D'Odorico, S. 1991, A&A, 251, 92